

Optically switchable photonic metasurfaces

R. F. Waters,¹ P. A. Hobson,² K. F. MacDonald,¹ and N. I. Zheludev^{1,3}

¹Centre for Photonic Metamaterials and Optoelectronics Research Centre, University of Southampton, Southampton SO17 1BJ, United Kingdom

²QinetiQ Ltd., Cody Technology Park, Farnborough, Hampshire GU14 0LX, United Kingdom

³Centre for Disruptive Photonic Technologies and The Photonics Institute, Nanyang Technological University, Singapore 637371, Singapore

(Received 13 July 2015; accepted 11 August 2015; published online 24 August 2015)

We experimentally demonstrate an optically switchable gallium-based metasurface, in which a reversible light-induced transition between solid and liquid phases occurring in a confined nanoscale surface layer of the metal drives significant changes in reflectivity and absorption. The metasurface architecture resonantly enhances the metal's "active plasmonic" phase-change nonlinearity by an order of magnitude, offering high contrast all-optical switching in the near-infrared range at low, $\mu\text{W } \mu\text{m}^{-2}$, excitation intensities. © 2015 AIP Publishing LLC.

[<http://dx.doi.org/10.1063/1.4929396>]

Photonic metamaterials were conceived and first realized as a means of achieving exotic optical properties, such as negative refractive index and optical frequency magnetism, not available in nature. They have evolved rapidly into a functional platform for the engineering of nanoscale photonic "meta-devices"¹ offering a wide range of switchable, tuneable, and nonlinear properties, typically achieved by hybridizing a plasmonic metal resonator framework with an active medium. Among the latter, phase-change media such as chalcogenide glasses,^{2,3} vanadium dioxide,^{4,5} and liquid crystals^{6–8} have been shown experimentally to offer substantial excitation-induced changes in optical properties, including nonvolatile all-optical switching functionality in the chalcogenide case.⁹ In the context of nonlinearity, metamaterial and metasurface nanostructures have been employed to resonantly amplify the response of conventional intrinsically nonlinear media via local field enhancement effects and/or arrangements of constituent elements that enhance efficiency (esp. phase-matching for harmonic generation).¹⁰ But they also provide mechanisms, via reversible mechanically-, thermally-, electrically-, magnetically-, and optically-induced changes in the composition and/or configuration of unit cells, which can deliver effective optical nonlinearities orders of magnitude larger than those found in bulk media.¹¹ Here, we harness an optically induced interfacial phase transition in the plasmonic metal framework of a planar metamaterial—the gallium backplane of a metamaterial "perfect absorber"—to drive reversible changes in its spectral response and thereby to provide a large, resonantly enhanced, effective optical nonlinearity.

Gallium is a remarkably polymorphic element, existing in up to nine different phases with properties ranging from those of the liquid, which is a highly reflective, near-ideal free-electron metal at optical frequencies,^{12,13} to those of the α phase—the stable bulk solid form, which is less "metallic" in character (less reflective, more absorbing) as a consequence of the low free-electron density in its partially covalently bound orthorhombic crystal structure.^{14,15} An unusually large change in optical properties is thus associated with solid-liquid transitions in gallium ($|\epsilon_l - \epsilon_s| \sim 90$ at

a wavelength of $1 \mu\text{m}$, ϵ_l and ϵ_s being, respectively, the complex relative permittivities of liquid and polycrystalline solid gallium), which has a bulk melting point T_m of 29.8°C . Gallium also exhibits strong surface melting behavior, whereby at an interface between the solid α -phase and a dielectric, surface energy considerations dictate the formation of a few-nm thick liquid layer even at temperatures several degrees below T_m .¹⁶ The thickness of this interfacial layer, and thereby the optical properties of the metal/dielectric interface are highly sensitive to both temperature and incident light intensity—in the latter case via both thermal and non-thermal transition mechanisms.^{17,18} These characteristics have seen gallium previously exploited in nonlinear mirrors for laser cavity Q-switching¹⁹ (cf. saturable absorbers), and for all-optical and "active plasmonic" signal modulation,^{20–22} including in the form of a gallium/aluminum metamaterial composite formed by grain boundary penetration.²¹ Indeed, the term "active plasmonic" itself was coined to describe functionality based upon gallium surface metallization.²³

Gallium's surface-mediated phase-change nonlinearity can readily be harnessed and resonantly enhanced in a photonic metamaterial "perfect absorber." Such structures, realized over recent years at progressively higher frequencies from the microwave²⁴ to near-infrared^{25,26} and optical domains,²⁷ generically comprise a planar array of sub-wavelength plasmonic metal resonators and a continuous metallic (mirror) backplane, separated by a thin dielectric spacer—the resonant absorption frequency being set by the relative permittivities of the constituent media, the geometry of the nanostructured metal layer, and thickness of the spacer.²⁸ Incorporating a gallium backplane mirror, as illustrated in Fig. 1(a), provides a mechanism for dynamically controlling the resonant response of the plasmonic metasurface with light, and delivers an order of magnitude enhancement of the metal's optical nonlinearity.

Experimental samples consist of a gold nano-disc array and silicon nitride spacer layer over the elemental gallium backplane. Gold disc arrays (Fig. 1(b)) (typically covering a $25 \mu\text{m} \times 25 \mu\text{m}$ area; ~ 5400 unit cells) are fabricated by

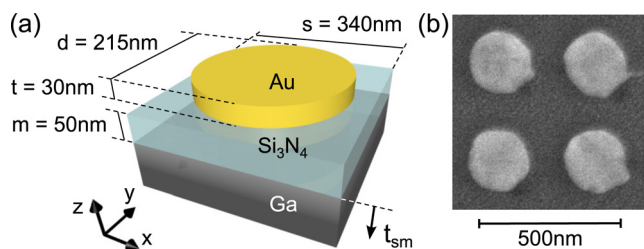


FIG. 1. (a) Artistic impression and unit cell design dimensions of a gallium-backplane/ Si_3N_4 /gold-disc metasurface absorber with a resonant wavelength of ~ 1310 nm. (b) Plan view scanning electron microscope image of a section of the fabricated gold disc array on silicon nitride.

focused ion beam milling in a 30 nm film of gold evaporated onto one side of a 50 nm thick $500 \mu\text{m} \times 500 \mu\text{m}$ silicon nitride membrane suspended in a silicon frame. The opposing side of the membrane is subsequently pressed into contact with a bulk liquid gallium droplet (6N purity), which is then cooled to produce an optically thick solid gallium/silicon nitride backplane mirror. Normal-incidence metasurface optical reflectivity spectra for the solid and liquid phase states of the gallium backplane (at sample temperatures T of 23.5 and 31.5 °C, respectively) were measured experimentally using a microspectrophotometer, and evaluated computationally in 3D finite element simulations. The numerical model employed material parameters for gold, liquid, and solid gallium from Refs. 29, 30, and 15, respectively, and a non-dispersive refractive index of 2.0 for the silicon nitride layer. It utilized periodic boundary conditions in the x and y directions and assumed normally incident, narrowband plane wave illumination. There is good quantitative agreement between experimental and computational spectra for the liquid phase of the gallium backplane, Fig. 2(a), but some discrepancy for the solid phase. This can in part be attributed to the small systematic spectral offset between experiment and simulation (including manufacturing imperfection and inhomogeneity in the gold disc array) also evident for the liquid phase; and to the likely persistence of a few-nm surface-melt layer between the solid gallium bulk and the silicon nitride (i.e., the solid phase model here should be considered a limiting case). Prior studies have inferred a preferred orientation for the orthorhombic gallium crystal at a silica interface;¹⁸ however, in the present case modelling shows that variations in crystal orientation are almost inconsequential to the spectral position or magnitude of the metasurface absorption resonance. We therefore represent the solid phase via a “polycrystalline” numerical average over the complex refractive indices for the three primary axes of α -gallium.

The metamaterial’s near-infrared absorption band corresponds to the dipolar gap plasmon resonance of the gold disc/mirror backplane combination,³¹ as illustrated by the surface charge density map inset to Fig. 2(a). Its spectral position and quality factor depend on the phase state of the gallium backplane and on the gold disc diameter d (Fig. 2(b)). The shorter (visible) wavelength reflectivity minimum corresponds to a Fabry-Pérot resonance, i.e., its spectral position is dictated by the effective optical thickness of the nitride layer and cannot be manipulated via adjustments of the gold pattern geometry.

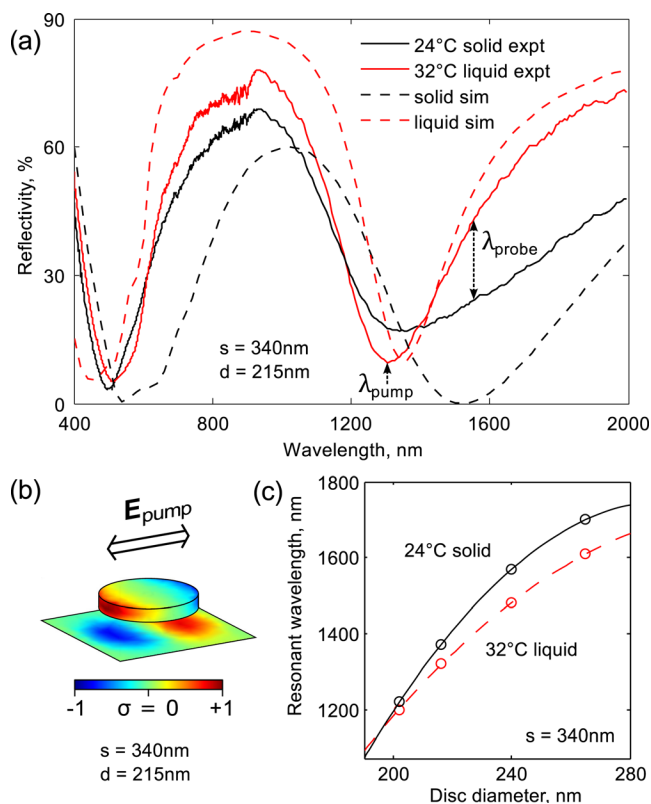


FIG. 2. (a) Experimental and numerically simulated reflectivity spectra for the gallium-backplane/ Si_3N_4 /gold-disc metasurface absorber of Fig. 1, for the solid [sample temperature $T = 23.5$ °C] and liquid [$T = 31.5$ °C] phase states of the gallium. (b) Computed relative surface charge density (σ) distribution on gold and gallium surfaces at 1330 nm liquid-phase absorption resonance [the arrow above denoting the incident light polarisation]. (c) Experimentally observed dependence of absorption resonance wavelength on gold nano-disc diameter at a fixed unit cell size $s = 340$ nm for the two phase states of the gallium backplane.

Reversible optical tuning of metasurface absorption underpinned by light-induced interfacial metallization of gallium was characterized using a near-infrared microscope configured, via a single laser input port, for dual-wavelength (1310 nm pump; 1550 nm probe) reflectivity measurements. A metasurface sample was engineered, with dimensions as presented in Fig. 1, to provide strong absorption at the 1310 nm pump wavelength and good reflectivity contrast between gallium phase states ($C = (R_{\text{max}} - R_{\text{min}})/R_{\text{min}}$) at 1550 nm, and mounted in a low pressure thermostatic stage (with sample temperature T being calibrated against the bulk melting point of gallium $T_m = 29.8$ °C). The two input beams, originating from single-mode fibre-coupled diode lasers, were focused to concentric spots on the sample with Gaussian intensity FWHM dimensions of $15.7 \mu\text{m}$ for the 1310 nm pump and $6.6 \mu\text{m}$ for the 1550 nm probe. The probe was maintained at a fixed CW intensity of $1.0 \mu\text{W} \mu\text{m}^{-2}$, while the pump was modulated at 500 Hz with 25% duty cycle (rise/fall times $< 1 \mu\text{s}$) at peak intensities up to $16.8 \mu\text{W} \mu\text{m}^{-2}$.

For a selection of fixed pump peak intensities, the time dynamics of the metasurface’s nonlinear 1550 nm reflective response were recorded while ramping the sample temperature, at a rate of 0.5 °C min^{-1} , from 0 to 32 °C (Fig. 3(a)). Under pump illumination the nanoscale layer of metallic gallium at the metal’s interface with silicon nitride grows to

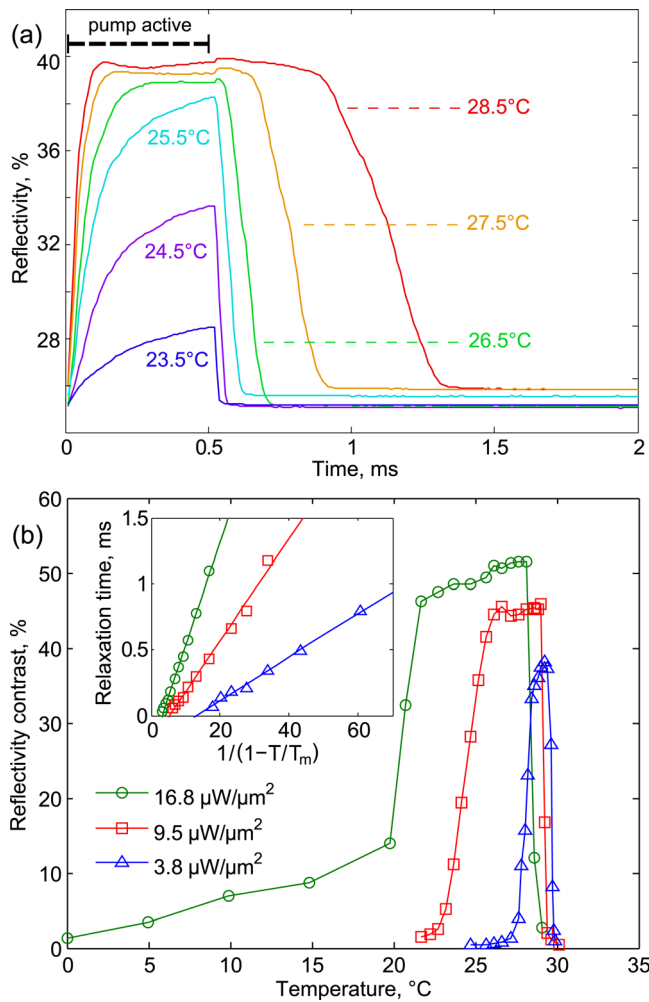


FIG. 3. (a) Absolute 1550 nm reflectivity of the gallium metasurface as a function of time during and after excitation with a 500 μs , 9.5 $\mu\text{W } \mu\text{m}^{-2}$ pump pulse at 1310 nm, for a selection of sample temperatures (as labelled) approaching the metal's bulk melting point (pump modulation frequency 500 Hz; traces averaged over 32 cycles). (b) Maximum induced 1550 nm reflectivity change for a selection of 1310 nm pump intensities (as labelled) as a function of sample temperature. The inset shows reflectivity relaxation time as a function of temperature and pump intensity.

an effective thickness t_s that increases with light intensity and with the proximity of sample temperature T to gallium's bulk melting temperature T_m .^{17,18} (In practice, metallization may proceed through the growth and aggregation of inclusions within the α -phase skin depth as opposed to the movement of a single solid/melt boundary.) The metasurface reflectivity increases as a result, towards a maximum intensity-dependent saturation level equal to its bulk liquid gallium backplane reflectivity level (a relative change of over 50% [Fig. 3(b)]), which is achieved when the excitation-enhanced surface melt layer becomes optically thick (the skin depth of liquid gallium at 1550 nm being ~ 19 nm). At lower intensities and sample temperatures, the induced reflectivity change accumulates throughout the 500 μs duration of the pump pulse as the illuminated sample area moves towards a metastable equilibrium state balancing the rates of light-induced metallization (via resonant absorption in the gallium and the gold leading to heating within the optical skin depth of gallium, and direct photo-excitation of covalent dimers within the α -gallium crystal structure^{17,18})

against the conductive removal of heat from the skin layer predominantly into the gallium bulk. At higher intensities and temperatures close to T_m , the surface metallization observable as a change in 1550 nm reflectivity proceeds more rapidly and the reflectivity level saturates within the pump pulse duration.

Relaxation time, defined as the interval between withdrawal of the pump excitation and recovery of the photoinduced reflectivity change to below 1/e of its maximum value, as the metallized surface layer of gallium reverts to the α -phase, increases critically towards T_m as shown in the inset to Fig. 3(b).

The phase transition-mediated nonlinear dependence of gallium metasurface reflectivity on incident light intensity cannot be quantified in terms of a conventional $\chi^{(3)}$ nonlinear susceptibility value nor indeed can one readily be approximated on the basis of the induced change in the metal's relative permittivity alone. However, a meaningful figure of merit γ may be obtained by considering the induced change in reflectivity per unit illumination intensity

$$\gamma = \frac{dR/R_0}{dI}, \quad (1)$$

where R_0 and R are the probe wavelength reflectivities at pump illumination intensity levels of zero and I , respectively. γ reaches a peak value of order 120 $\mu\text{m}^2 \text{ mW}^{-1}$ (a relative reflectivity change of 38% at an incident intensity of 3.8 $\mu\text{W } \mu\text{m}^{-2}$) for the gallium metasurface at a temperature of 28.8 $^\circ\text{C}$, one degree below T_m . This should be compared with the values of 17 $\mu\text{m}^2 \text{ mW}^{-1}$ for a simple planar mirror interface between gallium and a 50 nm silicon nitride membrane (evaluated as part of the present study) and a value of 24 $\mu\text{m}^2 \text{ mW}^{-1}$ for a planar gallium/silica interface at a wavelength of 810 nm (Ref. 17), both at $T = T_m - 1 = 28.8$ $^\circ\text{C}$.

Photonic metasurfaces with actively controllable, adaptive, and nonlinear spectral response functions offer applications potential in fields ranging from radiation emitters and sensors to spatial light modulators. The present study shows that gallium, as an active plasmonic medium undergoing optically induced surface metallization at low light intensities, provides unique functionality for cross-wavelength continuous tuning and switching of the spectral response of such structures, delivering in the present case a $>50\%$ relative change in 1550 nm reflectivity under $<20 \mu\text{W } \mu\text{m}^{-2}$ illumination at 1310 nm. Indeed, the gallium metasurface achieves a nonlinear reflection coefficient, for pump and probe wavelengths selected by design, which is an order of magnitude larger than that of the corresponding unstructured gallium/dielectric interface.

This work was supported by The Defence Science and Technology Laboratory (Dstl) through the Materials And Structures Technology (MAST) Programme, the Engineering and Physical Sciences Research Council (EPSRC) [Grant No. EP/G060363/1], and the Singapore Ministry of Education [Grant no. MOE2011-T3-1-005]. Following a period of embargo, the data from this paper can be obtained from the University of Southampton ePrints research repository, doi:10.5258/SOTON/378810.

- ¹N. I. Zheludev and Y. S. Kivshar, *Nat. Mater.* **11**, 917 (2012).
- ²Z. L. Sámson, K. F. MacDonald, F. De Angelis, B. Gholipour, K. Knight, C. C. Huang, E. Di Fabrizio, D. W. Hewak, and N. I. Zheludev, *Appl. Phys. Lett.* **96**, 143105 (2010).
- ³A. K. U. Michel, D. N. Chigrin, T. W. W. Maß, K. Schönauer, M. Salinga, M. Wuttig, and T. Taubner, *Nano Lett.* **13**, 3470 (2013).
- ⁴T. Driscoll, H.-T. Kim, B.-G. Chae, B.-J. Kim, Y.-W. Lee, N. M. Jokerst, S. Palit, D. R. Smith, M. Di Ventra, and D. N. Basov, *Science* **325**, 1518 (2009).
- ⁵M. J. Dicken, K. Aydin, I. M. Pryce, L. A. Sweatlock, E. M. Boyd, S. Walavalkar, J. Ma, and H. A. Atwater, *Opt. Express* **17**, 18330 (2009).
- ⁶S. Xiao, U. K. Chettiar, A. V. Kildishev, V. Drachev, I. C. Khoo, and V. M. Shalaev, *Appl. Phys. Lett.* **95**, 033115 (2009).
- ⁷B. Kang, J. H. Woo, E. Choi, H.-H. Lee, E. S. Kim, J. Kim, T.-J. Hwang, Y.-S. Park, D. H. Kim, and J. W. Wu, *Opt. Express* **18**, 16492 (2010).
- ⁸O. Buchnev, J. Y. Ou, M. Kaczmarek, N. I. Zheludev, and V. A. Fedotov, *Opt. Express* **21**, 1633 (2013).
- ⁹B. Gholipour, J. Zhang, K. F. MacDonald, D. W. Hewak, and N. I. Zheludev, *Adv. Mater.* **25**, 3050 (2013).
- ¹⁰M. Lapine, I. V. Shadrivov, and Y. S. Kivshar, *Rev. Mod. Phys.* **86**, 1093 (2014).
- ¹¹J. Valente, J. Y. Ou, E. Plum, I. Youngs, and N. I. Zheludev, *Nat. Commun.* **6**, 7021 (2015); J. Y. Ou, E. Plum, J. Zhang, and N. I. Zheludev, [arXiv:1506.05852](https://arxiv.org/abs/1506.05852) (2015); A. Karvounis, J. Y. Ou, K. F. MacDonald, and N. I. Zheludev, [arXiv:1508.00995](https://arxiv.org/abs/1508.00995) (2015).
- ¹²N. R. Comins, *Philosophical Magazine* **25**, 817 (1972).
- ¹³O. Hunderi and R. Ryberg, *J. Phys. F: Met. Phys.* **4**, 2096 (1974).
- ¹⁴M. Bernasconi, G. L. Chiarotti, and E. Tosatti, *Phys. Rev. B* **52**, 9988 (1995).
- ¹⁵R. Kofman, P. Cheyssac, and J. Richard, *Phys. Rev. B* **16**, 5216 (1977).
- ¹⁶G. Fritsch and E. Luscher, *Philos. Mag. A* **48**, 21 (1983).
- ¹⁷K. F. MacDonald, V. A. Fedotov, R. W. Eason, N. I. Zheludev, A. V. Rode, B. Luther-Davies, and V. I. Emel'yanov, *J. Opt. Soc. Am. B* **18**, 331 (2001).
- ¹⁸V. Albanis, S. Dhanjal, V. A. Fedotov, K. F. MacDonald, N. I. Zheludev, P. Petropoulos, D. J. Richardson, and V. I. Emel'yanov, *Phys. Rev. B* **63**, 165207 (2001).
- ¹⁹P. Petropoulos, H. L. Offerhaus, D. J. Richardson, S. Dhanjal, and N. I. Zheludev, *Appl. Phys. Lett.* **74**, 3619 (1999).
- ²⁰P. J. Bennett, S. Dhanjal, P. Petropoulos, D. J. Richardson, N. I. Zheludev, and V. I. Emel'yanov, *Appl. Phys. Lett.* **73**, 1787 (1998).
- ²¹A. V. Krasavin, K. F. MacDonald, N. I. Zheludev, and A. V. Zayats, *Appl. Phys. Lett.* **85**, 3369 (2004).
- ²²S. R. C. Vivekchand, C. J. Engel, S. M. Lubin, M. G. Blaber, W. Zhou, J. Y. Suh, G. C. Schatz, and T. W. Odom, *Nano Lett.* **12**, 4324 (2012).
- ²³A. V. Krasavin and N. I. Zheludev, *Appl. Phys. Lett.* **84**, 1416 (2004).
- ²⁴V. A. Fedotov, P. L. Mladyonov, S. L. Prosvirnin, and N. I. Zheludev, *Phys. Rev. E* **72**, 1 (2005).
- ²⁵J. Hao, J. Wang, X. Liu, W. J. Padilla, L. Zhou, and M. Qiu, *Appl. Phys. Lett.* **96**, 251104 (2010).
- ²⁶N. Liu, M. Mesch, T. Weiss, M. Hentschel, and H. Giessen, *Nano Lett.* **10**, 2342 (2010).
- ²⁷K. Aydin, V. E. Ferry, R. M. Briggs, and H. A. Atwater, *Nat. Commun.* **2**, 517 (2011).
- ²⁸C. M. Watts, X. Liu, and W. J. Padilla, *Adv. Mater.* **24**, OP98 (2012).
- ²⁹E. D. Palik, *Handbook of Optical Constants of Solids* (Elsevier, 1998).
- ³⁰R. S. Teshev and A. A. Shebzukhov, *Opt. Spectrosc. (USSR)* **65**, 693 (1988).
- ³¹A. Pors, O. Albrektsen, I. P. Radko, and S. I. Bozhevolnyi, *Sci. Rep.* **3**, 1 (2013).